MOLECULAR AND CELLULAR BIOLOGY, Mar. 2008, p. 1669–1678 Vol. 28, No. 5
0270-7306/08/$08.00+0 doi:10.1128/MCB.00891-07

Early Embryonic Lethality of Mice Lacking ZO-2, but Not ZO-3, Reveals Critical and Nonredundant Roles for Individual Zonula Occludens Proteins in Mammalian Development[▽]†

Jianliang Xu, P. Jaya Kausalya, Dominic C. Y. Phua, Safiah Mohamed Ali, Zakir Hossain, and Walter Hunziker*

Epithelial Cell Biology Laboratory, Institute of Molecular and Cell Biology, Agency for Science, Technology and Research, 61 Biopolis Drive, Singapore 138673, Republic of Singapore

Received 19 May 2007/Returned for modification 22 June 2007/Accepted 10 December 2007

ZO-1, ZO-2, and ZO-3 are closely related scaffolding proteins that link tight junction (TJ) transmembrane proteins such as claudins, junctional adhesion molecules, and occludin to the actin cytoskeleton. Even though the zonula occludens (ZO) proteins are among the first TJ proteins to have been identified and have undergone extensive biochemical analysis, little is known about the physiological roles of individual ZO proteins in different tissues or during vertebrate development. Here, we show that *ZO-3* knockout mice lack an obvious phenotype. In contrast, embryos deficient for ZO-2 die shortly after implantation due to an arrest in early gastrulation. *ZO-2*$^{-/-}$ embryos show decreased proliferation at embryonic day 6.5 (E6.5) and increased apoptosis at E7.5 compared to wild-type embryos. The asymmetric distribution of prominin and E-cadherin to the apical and lateral plasma membrane domains, respectively, is maintained in cells of *ZO-2*$^{-/-}$ embryos. However, the architecture of the apical junctional complex is altered, and paracellular permeability of a low-molecular-weight tracer is increased in *ZO-2*$^{-/-}$ embryos. Leaky TJs and, given the association of ZO-2 with connexins and several transcription factors, effects on gap junctions and gene expression, respectively, are likely causes for embryonic lethality. Thus, ZO-2 is required for mouse embryonic development, but ZO-3 is dispensable. This is to our knowledge the first report showing that an individual ZO protein plays a nonredundant and critical role in mammalian development.

Tight junctions (TJs) are regions of intimate contact between the plasma membrane domains of adjoining cells and are predominantly found in columnar epithelial and endothelial cells, where they are part of the apical junctional complex (reviewed in reference 47). TJs are also found in hepatocytes (13), keratinocytes (13), and Schwann cells (40).

TJs contain integral membrane proteins, notably claudins, occludin, and junctional adhesion molecules, which engage in homotypic and heterotypic interactions through their extracellular domains with corresponding proteins on adjoining cells (reviewed in reference 3 and 52). On the cytoplasmic side, adaptor or scaffolding molecules tether the integral membrane TJ proteins to the actin cytoskeleton. The best-characterized adaptors that directly link transmembrane TJ proteins to the cytoskeleton are ZO-1, ZO-2, and ZO-3, three closely related proteins that are widely expressed in different tissues and organs (reviewed in reference 21). Zonula occludens (ZO) proteins carry three PDZ (PSD-95/Dlg/ZO-1) domains, an Src homology 3 domain, and a guanylate kinase-like domain, and hence belong to the membrane-associated guanylate kinase-like superfamily of proteins (reviewed in references 20 and 21). A growing number of both structural and regulatory proteins that associate with the different domains of ZO proteins have been identified (reviewed in reference 21). Some of these interacting partners bind selectively to an individual ZO protein; others bind to two or even all three family members.

Several functions have been associated with TJs. On one hand, TJs are thought to restrict the diffusion of integral membrane proteins and outer leaflet lipids between different plasma membrane domains, for example, the apical and basolateral surfaces of columnar epithelial cells. On the other hand, TJs function as charge- and size-selective paracellular pores, providing barriers between the external and internal milieu of organs or establishing tissue compartments with distinct electrolyte compositions within organs (reviewed in references 2, 31, 47, 52, and 53). Recent evidence also indicates that TJs participate in the regulation of vesicular membrane transport (reviewed in reference 31) and cell differentiation and proliferation (reviewed in references 35 and 36).

The precise relevance of individual ZO proteins with respect to TJ assembly and functions remains largely unknown. Components of TJs, including ZO family members, can be incorporated into adherens junctions, gap junctions, and the intercalated discs of cardiomyocytes (9), suggesting that they play additional roles in cell-cell adhesion and intercellular communication. Furthermore, it is not clear if the three ZO family members are functionally redundant or if they each are linked to specific functions. Inactivation of ZO-1 by homologous recombination in mammary Eph4 cells revealed only minor defects, including a retarded recruitment of claudins and occludin to TJs, delayed barrier establishment, and the loss of cingulin from TJs (49). Exogenous expression of ZO-1, but not

* Corresponding author. Mailing address: Institute of Molecular and Cell Biology, 61 Biopolis Drive, Singapore 138673, Republic of Singapore. Phone: 65 6586 9599. Fax: 65 6779 1117. E-mail: hunziker@imcb.a-star.edu.sg.

† Supplemental material for this article may be found at http://mcb.asm.org/.

▽ Published ahead of print on 2 January 2008.

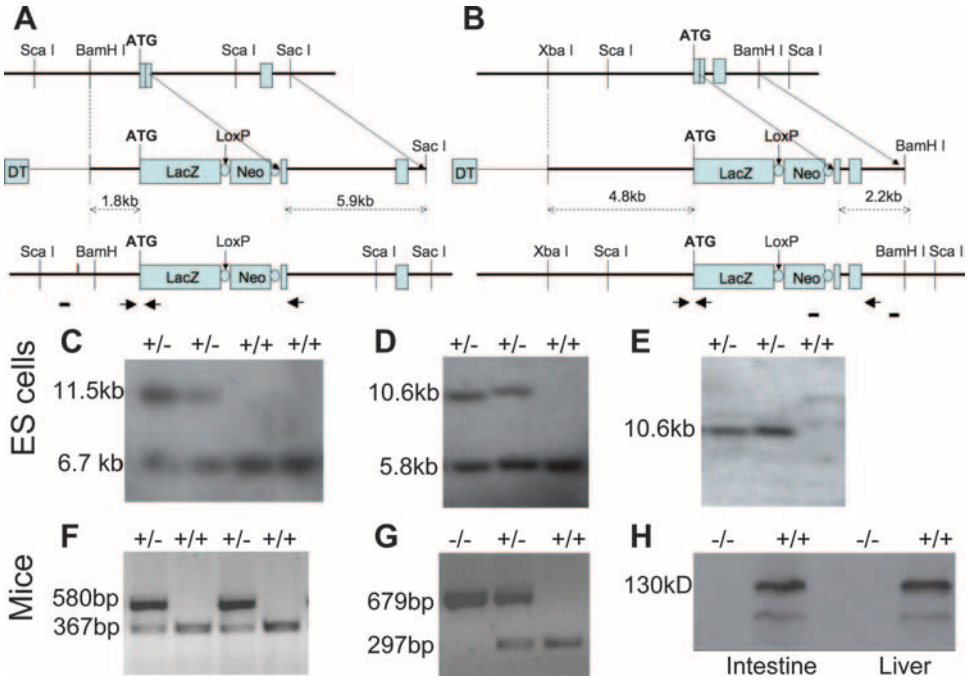

FIG. 1. Targeting of the *ZO-2* and *ZO-3* loci and genotyping. (A and B) Targeting strategy. Schematic representations of the genomic locus of *ZO-2* (A) and *ZO-3* (B) showing exon 2 (with the initiation ATG) and exon 3 (gray boxes). The targeting vectors are designed to disrupt exon 2 by the in-frame insertion of a *lacZ* gene and a *loxP*-flanked neomycin cassette immediately downstream of the ATG codon. Bars indicate the regions to which probes used for Southern blot analysis hybridize; arrows denote the regions where primers used for genotyping anneal. (C to E) Homologous recombination in ESCs. Southern blot of ScaI-digested genomic DNA of selected ESC clones hybridized with labeled DNA probes hybridizing to genomic DNA (C and D) or the neomycin gene (E), as described in panels A and B, for the identification of homologous recombinants. ScaI fragments of 11.5- and 6.7-kb (*ZO-2*) or 10.6- and 5.8-kb (*ZO-3*) corresponding to the WT and targeted mutant alleles, respectively, are detected in targeted (+/−) ESC clones, whereas only the fragment corresponding to the WT allele is present in controls (+/+). (F and G) Genotyping of transgenic mice. Genomic DNA was amplified by PCR using primers designed to distinguish between WT and mutant alleles, as described in panels A and B. Fragments of 580 bp are 679 bp are indicative of the presence of the recombined mutant allele of *ZO-2* and *ZO-3*, respectively, while the 367-bp and 297-bp fragments denote the WT allele. No $ZO\text{-}2^{-/-}$ mice were detected in newborn litters. (H) Western blot detection of ZO-3 protein. Lysates of intestine and liver from postnatal day 9 $ZO\text{-}3^{+/+}$ and $ZO\text{-}3^{-/-}$ littermates were fractionated by SDS-polyacrylamide gel electrophoresis, transferred to membranes, and blotted with antibodies to ZO-3.

ZO-2, rescued the observed phenotype, suggesting that despite redundancy for junction establishment and epithelial polarization, the two ZO proteins may not be functionally identical. Similarly, in MDCK cells, where ZO-1 expression was silenced using small interfering RNA (siRNA), the formation of TJs was delayed, but they eventually matured to full functionality (37). Depletion of ZO-2 using siRNA had no discernible effects on TJ structure or function in Eph4 (48) cells. In MDCK cells, silencing of ZO-2 had either no effect (38) or, as reported in a recent study (23), resulted in a compromised barrier, the apical mislocalization of E-cadherin, and widened intracellular spaces. Furthermore, while in MDCK cells the absence of ZO-2 did not increase the delay in TJ formation caused by the lack of ZO-1 (37), it had dramatic effects on TJ formation in Eph4 cells lacking ZO-1 (48). Eph4 cells deficient for both ZO-1 and ZO-2 lacked morphologically discernible TJs and showed a loss of paracellular barrier function and a failure to concentrate Cldn-3, occludin, and the junctional adhesion molecule at cellular junctions, but they retained epithelial polarization. In the case of ZO-3, TJ structure and function were unaffected in ZO-3-deficient cells, and even the additional suppression of ZO-2 by siRNA failed to affect TJ architecture (1).

To explore the physiological role of ZO proteins in vivo during development and in different organs, we have inactivated by homologous recombination each of the corresponding genes in mice. Here we report on the generation of *ZO-2* and *ZO-3* knockout (KO) mice. $ZO\text{-}3^{-/-}$ mice showed no apparent phenotype, in accordance with a recent report (1). Interestingly, however, $ZO\text{-}2^{-/-}$ mice suffered early embryonic lethality, establishing nonredundant functions for ZO-2 and ZO-3 and revealing a critical role for ZO-2 in mammalian embryonic development.

MATERIALS AND METHODS

Generation of ZO-2 and ZO-3 KO mice. Genomic fragments containing the *ZO-2* or *ZO-3* locus were isolated from a mouse 129SvJ genomic library (Stratagene) and subcloned into pBluescript II KS(+) (Stratagene). Targeting vectors were designed to replace the exon containing the start ATG of ZO-2 and ZO-3 and contained a *LacZ neo* cassette flanked by short and long arms of 1.8 kb and 5.9 kb, respectively, for *ZO-2* and 2.2 kb and 4.8 kb, respectively, for *ZO-3* (Fig. 1). The targeting vectors were linearized and electroporated into W4 embryonic stem cells (ESCs) (Taconic). G418-resistant clones were screened by PCR and Southern blot analysis. $ZO\text{-}2^{-/+}$ and $ZO\text{-}3^{-/+}$ ESC clones were injected into blastocysts derived from C57BL/6 mice to generate chimeras. Since germ line transmission was only obtained for one $ZO\text{-}2^{-/+}$ ESC clone, genomic integrity was verified by G-banding (data not shown). Furthermore, $ZO\text{-}2^{+/-}$ mouse

embryonic fibroblasts showed a normal kryotype (chromosome number and G-banding) (data not shown).

Genotyping by PCR analysis. Genomic DNA isolated from tail clippings or embryo tissue and suitable primers were used in a PCR for genotyping. Primer 1 (5′-ATGGAGGAGGTGATATGGGAGCAG-3′) and primer 2 (5′-TGTGTC ATTGGTGTGTGGAAGGAG-3′) were used amplify a fragment of 367 bp for the wild-type (WT) allele, whereas primer 3 (5′-GAGCTGTGTGGAAGCATA CCTAGT-3′) and primer 4 (5′-ATGGGATAGGTTACGTTGGTGTAG-3′) yielded a 580-bp product for the mutant allele of *ZO-2*. For *ZO-3*, primer 5 (5′-GAGGTATAGTGGGTAAGCCAGACA-3′) and primer 6 (5′-AAGGCGT TACTTCTCAGACCC AG-3′) amplified a 297-bp fragment for the WT allele, whereas primer 7 (5′-GAGGTATAGTGGGTAAGCCAGALA-3′) and primer 8 (5′-ATGGGATAGGTTACGTTGGTGTAG-3′) resulted in a 679-bp product for the mutant allele.

Southern blot analysis. Genomic DNA was extracted from G418-resistant ESCs and digested to completion with ScaI. For the *ZO-2* locus, a 566-bp fragment corresponding to the 5′ end or the right arm of the target vector (Fig. 1A) was labeled with [^{32}P]dCTP by random priming (Roche) and used as a probe. Fragments of 679 bp and 668 bp corresponding to the 3′ end of the left arm of the targeting vector and the Neo sequence, respectively, were labeled and used as probes for the *ZO-3* locus.

Histological analysis. Embryos at embryonic day 5.5 (E5.5), E6.5, E7.5, and E8.5 were isolated together with their deciduas from the uterus of pregnant mice. The embryos and deciduas were fixed in 4% paraformaldehyde overnight, embedded in paraffin, sectioned, and stained with hematoxylin and eosin. The slides were viewed with a Leica DM4000 B microscope, and the photos were taken with a DFC300 FX camera. To genotype embryos, tissue was microdissected from paraffin sections and digested in 20 μl of water containing 10 μg of proteinase K (Roche) at 56°C for 2 h. Proteinase K was then inactivated at 80°C for 10 min, and 2 μl of the digest was used for PCR analysis.

Immunostaining. Deciduas isolated from uteruses were fixed with 4% paraformaldehyde for 2 h to overnight, followed by washing with phosphate-buffered saline (PBS). The samples were kept in 20% sucrose overnight, transferred to solution containing equal parts 20% sucrose and 22-oxyacalcitriol for 4 h, frozen in 22-oxyacalcitriol, and then processed on a cryostat to obtain 5-μm thick sections. Immunostaining was carried out with rabbit polyclonal antibodies against ZO-1, ZO-2, ZO-3, occludin (Zymed), or the mesoderm marker T gene (Brachyury; Abcam) and with rat polyclonal antibodies against E-cadherin (Zymed) or prominin (eBioscience).

Isolation and culture of blastocysts in vitro. *ZO-2* heterozygote males and females were crossed, and the blastocysts were collected at 3.5 days postcoitus by flushing the uterus of plugged females with M2 medium (Sigma). Flushed blastocysts were then cultured individually in Dulbecco's modified Eagle's medium supplemented with 20% fetal bovine serum in 96-well plates at 37°C in 5% CO_2.

Generation of ZO-2 null ESCs. Independent *ZO-2*$^{+/-}$ ESCs were seeded in a six-well plate, and after 2 days they were trypsinized and replated onto a 10-cm dish and selected in 20 mg/ml G418 (Calbiochem). After 7 to 9 days of selection, drug-resistant colonies were picked. Half of the cells from each clone were screened by PCR, and the rest were expanded on feeder cells. *ZO-2*$^{-/-}$ ESC clones were amplified, and the absence of ZO-2 protein was confirmed by Western blotting. Eight independent *ZO-2* null ESC clones were obtained from two independent *ZO-2* heterozygous founder ESC clones.

Lanthanum permeability. E7.5 embryos and day 5 embryoid bodies (EBs) were immediately fixed in freshly made 2.5% glutaraldehyde for 1 to 3 h. In some experiments, WT EBs were incubated with 10 mM EGTA for 30 min on ice prior to fixation. After a rinse with PBS, the samples were postfixed in 1% osmium tetroxide containing 1% lanthanum nitrate for 1 h, rinsed in PBS, and processed for transmission electron microscopy as described below.

Transmission electron microscopy. E6.5 and E7.5 embryos were dissected from their deciduas and fixed in 2.5% glutaraldehyde. After a rinse with 0.1 M PBS, the embryos were postfixed in 1% osmium tetroxide for 1 h, rinsed in phosphate buffer, dehydrated in ethanol, and embedded in resin. Ultrathin sections were cut with a diamond knife, stained with uranyl acetate and lead citrate, and then viewed with a transmission electron microscope (JEM-1010).

Apoptosis assay. Terminal deoxynucleotidyltransferase-mediated dUTP-biotin nick end labeling (TUNEL) assays were performed on cryosections of mouse embryos from E6.5 to E8.5 with a TMR Red In Situ Cell Death Detection Kit (Roche), according to the manufacturer's protocol.

BrdU labeling. One hour before the mice were sacrificed, 100 μg of bromodeoxyuridine (BrdU; Sigma) per gram of body weight was injected peritoneally into the pregnant females. Deciduas were removed and treated as described above. The sections were stained with the in situ cell proliferation kit FLUOS (Roche) according to the manufacturer's protocol.

Western blot analysis. ESCs or EBs were washed twice in PBS and lysed for 15 min in radioimmunoprecipitation assay buffer (1% deoxycholate, 1% Triton X-100, 0.5% sodium dodecyl sulfate [SDS], 50 mM Na_2HPO_4, 150 mM NaCl, 2 mM EDTA) on ice. Lysates were cleared by centrifugation (13,000 × *g* for 15 min) at 4°C. The supernatant was fractionated by SDS-polyacrylamide gel electrophoresis and Western blot analysis essentially as described previously (29). No full-length ZO-2 or truncated fusion protein(s) was detected using antibodies to either the N-terminal linker region between PDZ2 and PDZ3 (sc-11448; Santa Cruz) or the C terminus (catalog number 38-9160; Zymed) of ZO-2.

RESULTS

Targeting of the ZO-2 and ZO-3 genes and generation of ZO-2 and ZO-3 KO mice. The *ZO-2* or *ZO-3* locus was targeted in W4 ESCs with a β-galactosidase gene (*lacZ*) knock-in targeting vector using the strategies outlined in Fig. 1A and B. Using this approach, the *lacZ* gene was placed in frame downstream of the initiation ATG of the *ZO-2* or *ZO-3* gene, resulting in a null mutation of the corresponding gene. ESCs were selected in G418, and clones were screened for homologous recombination at the *ZO-2* or *ZO-3* locus using Southern blot hybridization (Fig. 1C to E) and the probes indicated in Fig. 1A and B. Using gene-specific probes and genomic DNA digested with ScaI, 6.7-kb and 11.5-kb (Fig. 1C, *ZO-2*) and 5.8-kb and 10.6-kb bands (Fig. 1D, *ZO-3*) were detected for the WT and mutant alleles, respectively. As expected, the *neo*-specific probe hybridized only with the 10.6-kb band of *ZO-3*$^{+/-}$ ESCs (Fig. 1E). Homologous recombination was obtained in 2 (*ZO-2*) and 5 (*ZO-3*) out of 96 selected ESCs.

Correctly targeted ESC clones were injected into C57BL/6 blastocysts, and one clone each produced chimeric mice with germ line transmission of the mutated *ZO-2* and *ZO-3* alleles. Chimeras were mated with either C57BL/6 or 129 strain mice to establish the F_1 generation of heterozygous mice. Embryos or mice were routinely genotyped by PCR using the primers shown in Fig. 1A and B, resulting in 580-bp and 679-bp diagnostic fragments indicative of the mutated *ZO-2* (Fig. 1F) and *ZO-3* (Fig. 1G) alleles, respectively. *ZO-2* and *ZO-3* heterozygous mice were apparently normal and mated to obtain homozygous animals.

Embryonic lethality for *ZO-2*$^{-/-}$ but not *ZO-3*$^{-/-}$ mice. *ZO-3*$^{-/-}$ mice (Fig. 1G) were born according to Mendelian ratios. Of 97 offspring from matings of *ZO-3*$^{+/-}$ × *ZO-3*$^{+/-}$ mice, 23 were *ZO-3*$^{-/-}$, 17 were WT, and 57 were *ZO-3*$^{+/-}$. Embryonic development of *ZO-3*$^{-/-}$ mice was normal, and adult animals showed no apparent phenotype. ZO-3 protein, detected as a 130-kDa band by Western blotting and abundantly expressed in the intestines and livers of WT mice, could not be detected in tissues of *ZO-3*$^{-/-}$ animals (Fig. 1H), confirming the inactivation of the *ZO-3* locus. The loss of ZO-3 expression in the KO mice was further corroborated by immunolabeling. ZO-3, present on TJs of intestinal epithelial cells of control animals, was absent from the intestine of *ZO-3*$^{-/-}$ mice (Fig. 2A and B). No differences in the lateral localization of E-cadherin (Fig. 2C and D) or TJ morphology as assessed by transmission electron microscopy (Fig. 2E and F) were observed between control and *ZO-3*$^{-/-}$ intestinal epithelial cells. Preliminary analysis of our *ZO-3*$^{-/-}$ mice (Fig. 2 and data not shown) is in agreement with a recent detailed characterization of independently generated *ZO-3*$^{-/-}$ mice and derived teratocarcinoma cell lines, which also failed to establish a phenotype (1).

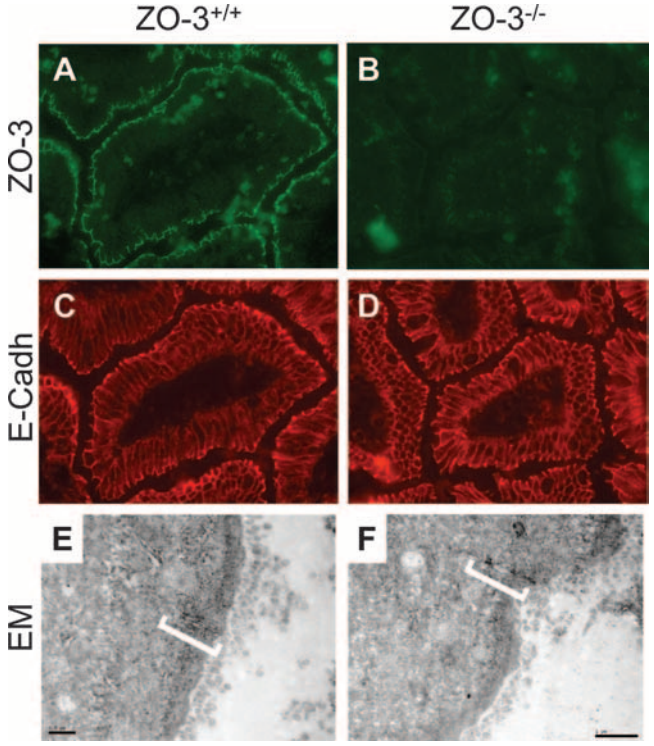

FIG. 2. E-cadherin expression and TJ morphology in intestinal epithelial cells of *ZO-3*$^{-/-}$ mice. (A to D) ZO-3 expression and E-cadherin localization. Sections of intestines from *ZO-3*$^{+/+}$ or *ZO-3*$^{-/-}$ littermates were stained with antibodies to ZO-3 (A and B) or E-cadherin (C and D) and fluorescently labeled secondary antibodies. (E and F) TJ morphology. Electron micrographs (EM) of intestinal sections of *ZO-3*$^{+/+}$ and *ZO-3*$^{-/-}$ mice showing the electron-dense plaques of the apical junctional complex between adjacent epithelial cells. Bars, 0.5 μm (E) and 1 μm (F).

In contrast to *ZO-3*$^{-/-}$ mice, however, *ZO-2*$^{-/-}$ offspring were absent in litters from *ZO-2* heterozygous crossings (Fig. 1F and Table 1), pointing to embryonic lethality. Genotyping of embryos from *ZO-2* heterozygous crossings at different developmental stages showed a gradual decline in the fraction of homozygous embryos (Table 1), and histological analysis revealed a concomitant increase in the number of small, abnormal embryos apparently undergoing resorption (Fig. 3). Dissection of embryos at E6.5, E7.5, and E8.5 confirmed their grossly underdeveloped and abnormal state compared to corresponding WT embryos (Fig. 4). Embryonic lethality was also observed in a pure Sv129 background. This and the normal karyotype (chromosome number and G-banding) (data not shown) of *ZO-2*$^{+/-}$ mouse embryonic fibroblasts make it un-

TABLE 1. Genotyping of offspring from *ZO-2*$^{+/-}$ × *ZO-2*$^{+/-}$ mating

Stage	Genotype (no. of embryos)[a]					
	WT	*ZO-2*$^{+/-}$	*ZO-2*$^{-/-}$			Total
			Abn	Res	Total	
Weaning	27	53			0	80
E9.5–E18.5	14	29	0	11	11	54
E8.5	7	12	3	1	4	23
E7.5	ND	ND	22	35	57	211
E6.5	ND	ND	19	15	34	141
E5.5	ND	ND	3	1	4	14
E3.5	16	37	0	0	15	68

[a] Genomic DNA of embryos at the indicated developmental stages was amplified by PCR using primers designed to distinguish between WT and mutant alleles (Fig. 1A and B). No *ZO-2*$^{-/-}$ mice were detected in newborn litters. ND, genotype not determined but size and morphology normal; Abn, abnormal morphology and small size; Res, resorbed and empty decidua.

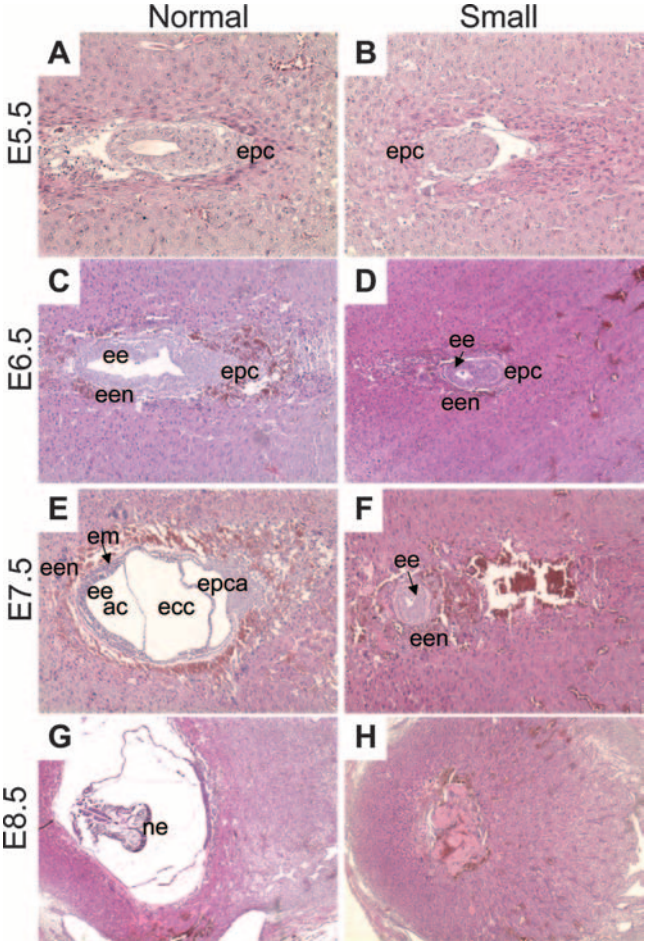

FIG. 3. Postimplantation development of *ZO-2*$^{-/-}$ embryos. Histology of embryos with typical normal or abnormal appearance at E5.5 (A and B), E6.5 (C and D), E7.5 (E and F), and E8.5 (G and H). Note the developmental arrest of *ZO-2*$^{-/-}$ embryos from E5.5 onwards and eventual resorption. epc, extraplacental cone; ac, amniotic cavity, ecc, exocoelomic cavity; epca, ectoplacental cavity; ne, neural ectoderm.

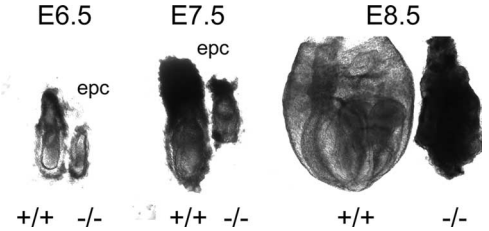

FIG. 4. Developmental arrest of *ZO-2*$^{-/-}$ embryos. *ZO-2*$^{+/+}$ and *ZO-2*$^{-/-}$ embryos dissected from their deciduas at E6.5, E7.5, and E8.5. Note the overall smaller size and developmental arrest of *ZO-2*$^{-/-}$ embryos. epc, extraplacental cone.

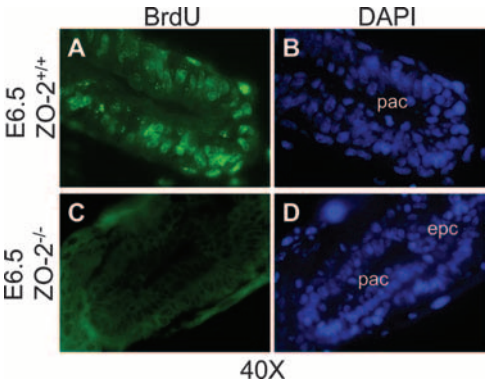

FIG. 5. Cell proliferation is compromised in E6.5 *ZO-2*$^{-/-}$ embryos. *ZO-2*$^{+/+}$ (A and B) and *ZO-2*$^{-/-}$ (C and D) E6.5 embryos were labeled with BrdU and incorporated BrdU (green; A and C), and nuclei (blue; B andD) were visualized in sections by fluorescence microscopy. pac, proamniotic cavity; epc, extraplacental cone.

likely that compromised genomic integrity is the cause for embryonic lethality of *ZO-2*$^{-/-}$ animals.

These findings thus establish a role for ZO-2 but not for ZO-3 in the embryonic development of mammals.

***ZO-2*$^{-/-}$ embryo development is compromised by reduced cell proliferation followed by apoptosis.** *ZO-2*$^{-/-}$ embryos appeared small and morphologically abnormal and failed to develop past the egg cylinder stage (Fig. 3). By E7.5, ZO-2$^{-/-}$ embryos were less than half the size of WT or heterozygous embryos (Fig. 4) and showed a general disorganization of embryo morphology and developmental defects such as an abnormal proamniotic cavity (Fig. 3C and D). Egg cylinders of *ZO-2*$^{-/-}$ embryos were composed of discreet ectoderm and endoderm cell layers but did not show morphological evidence of mesoderm development

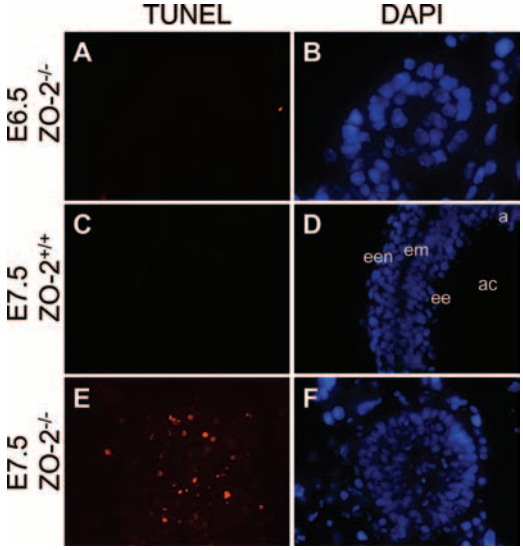

FIG. 6. Enhanced apoptosis in E7.5 *ZO-2*$^{-/-}$ embryos. Apoptosis in *ZO-2*$^{-/-}$ (A, B, E, and F) and *ZO-2*$^{+/+}$ (C and D) embryos at E6.5 (A and B) or E7.5 (C to F) was visualized by fluorescence microscopy using the TUNEL assay (red; A, C, and E). Nuclei are stained in blue (B, D, and F). a, amnion; ac, amniotic cavity; ee, embryonic ectoderm, em, embryonic mesoderm, een, embryonic endoderm.

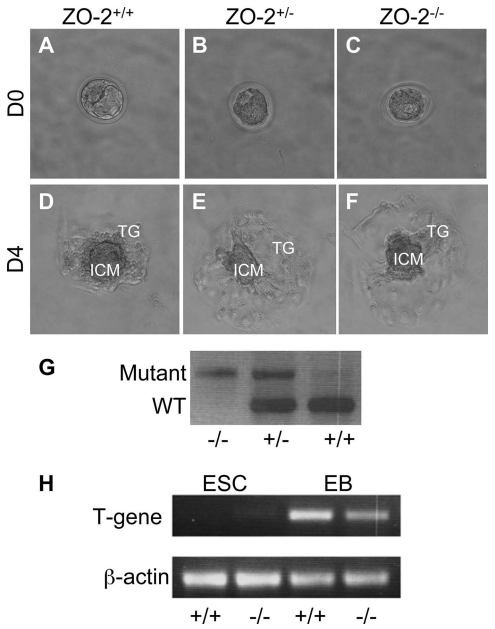

FIG. 7. *ZO-2*$^{-/-}$ blastocysts differentiate inner cell mass and trophoblast tissue in vitro and express the mesoderm marker T gene. (A to F) Blastocyst cultures. Micrographs of E3.5 *ZO-2*$^{+/+}$ (A and D), *ZO-2*$^{+/-}$ (B and E), or *ZO-2*$^{-/-}$ (C and F) blastocysts after isolation (day 0 [D0]) (A to C) or 4-day (D4) in vitro culture (D to F). Note the normal development of inner cell mass (ICM) and trophoblast outgrowth (TG) for *ZO-2*$^{-/-}$ blastocysts. (G) Genotyping. Blastocysts were genotyped by reverse transcription-PCR, yielding 367-bp and 580-bp fragments for the WT and inactivated *ZO-2* alleles, respectively. (H) T-gene expression. Reverse transcription-PCR was used to assess the expression of T gene in *ZO-2*$^{+/+}$ or *ZO-2*$^{-/-}$ ESCs and EBs.

(Fig. 3), consistent with the lack of staining for the mesoderm marker T (Brachyury) (data not shown).

Given the smaller size and apparent degeneration of *ZO-2*$^{-/-}$ embryos between E6.5 and E7.5, we determined if alterations in cell proliferation and/or apoptosis contributed to developmental arrest. Based on the analysis of BrdU incorporation, cells in WT embryos showed high proliferative activity at E6.5 (Fig. 5A and B). In contrast, few if any proliferating cells were present in *ZO-2*$^{-/-}$ embryos at this stage (Fig. 5C and D). Little if any apoptotic activity was observed by TUNEL assay in WT E6.5 (data not shown) or E7.5 embryos (Fig. 6C and D). However, while programmed cell death occurred at low levels in *ZO-2*$^{-/-}$ embryos at E6.5 (Fig. 6A and B), extensive apoptosis was observed in these embryos at E7.5 (Fig. 6E and F). Thus, the viability of *ZO-2*$^{-/-}$ embryos was compromised due to the loss of cell proliferation and the induction of apoptosis between E6.5 and E7.5.

To explore the developmental potential of *ZO-2*$^{-/-}$ blastocysts, E3.5 embryos removed from pregnant females following heterozygous mating were cultured in vitro. A similar expansion of the inner cell mass and trophoblast outgrowth were observed from day 0 (Fig. 7A to C) to day 4 (Fig. 7D to F) for WT, *ZO-2*$^{+/-}$, and *ZO-2*$^{-/-}$ (Fig. 7G) blastocysts in culture.

As expected, T gene expression was absent in ESCs. Despite its absence in E7.5 *ZO-2*$^{-/-}$ embryos in vivo, T was expressed in cultured *ZO-2*$^{-/-}$ EBs (Fig. 7H). This observation suggests that the lack of mesoderm formation in *ZO-2*$^{-/-}$ blastocysts is

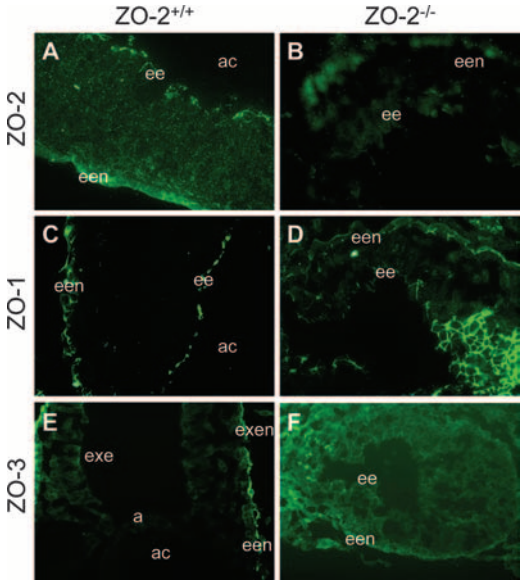

FIG. 8. Distribution of ZO-1 and ZO-3 in *ZO-2*$^{-/-}$ embryos is not altered. Sections of E7.5 *ZO-2*$^{+/+}$ (A, C, and E) and *ZO-2*$^{-/-}$ (B, D, and F) embryos were labeled with antibodies to ZO-2 (A and B), ZO-1 (C and D), or ZO-3 (E and F) and visualized by fluorescence microscopy. a, amnion; ac, amniotic cavity; ee, embryonic ectoderm; een, embryonic endoderm; exen, extraembryonic endoderm; exe, extraembryonic ectoderm.

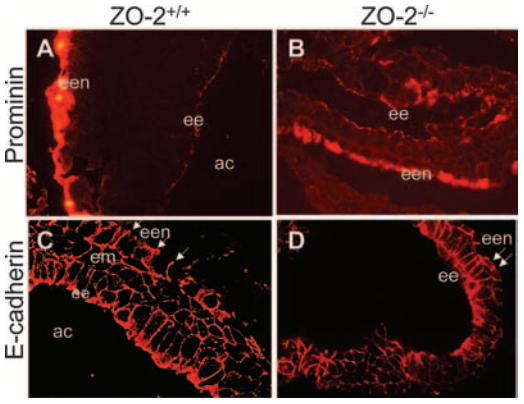

FIG. 9. Apical-basal polarity is not affected in *ZO-2*$^{-/-}$ embryos. Sections of E7.5 *ZO-2*$^{+/+}$ (A and C) and *ZO-2*$^{-/-}$ (B and D) embryos were labeled with antibodies to the apical marker prominin (A and B) and the lateral maker E-cadherin (B and D) and visualized by fluorescence microscopy. ac, amniotic cavity; ee, embryonic ectoderm; een, extraembryonic endoderm; ee, embryonic ectoderm; embryonic mesoderm.

due to apoptosis in the ectoderm layer rather than a requirement of ZO-2 for mesoderm induction per se.

Taken together, arrest of cell proliferation and subsequent programmed cell death between E6.5 and E7.5 prevent gastrulation in *ZO-2*$^{-/-}$ embryos.

The asymmetric distribution of plasma membrane proteins is not affected in cells of *ZO-2*$^{-/-}$ embryos. E7.5 embryos were stained with antibodies to ZO-2 to analyze its expression and distribution. ZO-2 was strongly expressed in WT embryos and enriched at sites of cell-cell contact of the extraembryonic and embryonic endoderm and ectoderm cell layers (Fig. 8A). As expected, no specific ZO-2 staining was obtained in *ZO-2*$^{-/-}$ embryos (Fig. 8B). E7.5 embryos also expressed ZO-1 and ZO-3, and both proteins were detected at the apical pole of cells of the extraembryonic and embryonic endoderm and ectoderm cell layers (Fig. 8C and E). ZO-3 expression was low in the embryonic ectoderm but high in the extraplacental cone. Neither the expression nor the distribution of ZO-1 or ZO-3 was significantly altered in *ZO-2*$^{-/-}$ embryos (Fig. 8D and F). Furthermore, no apparent difference in the apical localization of prominin (Fig. 9A and B) was observed between control and *ZO-2*-deficient E7.5 embryos. In *ZO-2*$^{+/+}$ embryos, E-cadherin was present in the lateral membrane of cells of the ectoderm and endoderm layers, with a concentration in the apical adhesion complexes in the ectoderm (Fig. 9C). The overall distribution of E-cadherin did not appear to be affected in the absence of ZO-2 (Fig. 9C and D).

These data indicate that the role of TJs in maintaining the asymmetric distribution of membrane proteins remained intact in cells of *ZO-2*$^{-/-}$ embryos.

The structure and permeability barrier of the apical junctional complex are altered in cells of *ZO-2*$^{-/-}$ embryos. To further assess the structural integrity of TJs, we analyzed E6.5 and E7.5 embryo sections by transmission electron microscopy. Electron-dense plaques characteristic of the apical junctional complex were readily detected at the apical pole of the lateral membrane of adjacent cells of the ectoderm cell layer of control embryos (Fig. 10A and C). In contrast, prominent elongated electron-dense plaques were rarely observed in cells of *ZO-2*$^{-/-}$ embryos (Fig. 10B and D). Quantification confirmed the presence of normal apical junctional plaques between most cells of control embryos, whereas cells of *ZO-2*$^{-/-}$ embryos presented only the occasional rudimentary plaque (Table 2).

Given the apparent structural alterations in TJs, we monitored paracellular permeability in *ZO-2*$^{-/-}$ embryos. Lanthanum permeability was efficiently restricted at the level of TJs in cells of control embryos (Fig. 10E and G). In contrast, lanthanum was readily detected in extracellular spaces between the lateral plasma membranes of adjacent cells of E7.5 *ZO-2*$^{-/-}$ embryos. Quantification showed that none of the TJs from control embryos allowed diffusion of lanthanum whereas more than 10% of the TJs from *ZO-2*$^{-/-}$ embryos were leaky (Table 3).

Thus, the structural and functional integrity of the apical junctional complex was compromised in cells of developing *ZO-2*$^{-/-}$ embryos.

Polarity, TJ structure, and paracellular permeability are unaffected in *ZO-2*$^{-/-}$ embryoid bodies. We next extended our analysis to EBs derived from either WT or *ZO-2* null ESCs. The second *ZO-2* allele was targeted in two independent *ZO-2*$^{+/-}$ ESC clones (see Fig. S1A in the supplemental material), including the clone used to generate the *ZO-2*$^{+/-}$ mice (see above). *ZO-2*$^{-/-}$ ESCs showed normal morphology (see Fig. S1B in the supplemental material). At 5 and 10 days of culture, *ZO-2*$^{+/-}$ EBs expressed approximately half the amount of ZO-2 protein compared to WT EBs, and, as expected from the design of the targeting vector, no expression of ZO-2 protein could be detected in *ZO-2*$^{-/-}$ EBs (see Fig. S1C in the supplemental material). Furthermore, Western blot analysis using a panel of antibodies to different regions of ZO-2 failed to

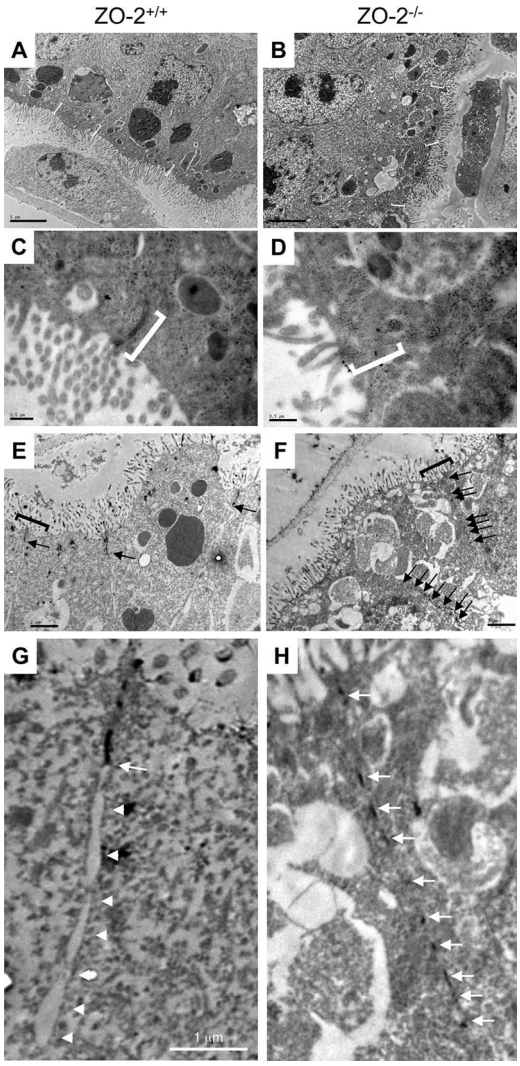

FIG. 10. The structure and permeability barrier of the apical junctional complex are altered in cells of *ZO-2*$^{-/-}$ embryos. (A to D) Structure. E6.5 (data not shown) and E7.5 embryo sections were analyzed by transmission electron microscopy to visualize the apical junctional complex. Typical electron-dense plaques were readily detected at the apical pole of the lateral membrane of adjacent cells of control embryos (A and C) but were rarely observed in cells of *ZO-2*$^{-/-}$ embryos (B and D). *ZO-2*$^{-/-}$ embryos were identified based on their small size compared to WT and heterozygous embryos. Bars, 5 μm (A and B) and 0.5 μm (C and D). (E and F) Lanthanum permeability. E7.5 embryos were postfixed in lanthanum nitrate and processed for transmission electron microscopy. Note the presence of lanthanum (black arrows) in intercellular spaces of *ZO-2*$^{-/-}$ (E) but not control (F) embryos. Bar, 2 μm. (G and H) Higher magnification of the TJs highlighted with square brackets in panels E and F. Bar, 1 μm.

detect truncated forms of ZO-2 (data not shown). Neither expression levels (see Fig. S2 and S3 in the supplemental material) nor localization of ZO-1 or ZO-3 was visibly altered in *ZO-2*$^{-/-}$ EBs (see Fig. S3 in the supplemental material). Analysis of selected TJ or adherens junction markers showed no changes in protein levels for occludin and cingulin or E-cadherin and β-catenin, respectively (see Fig. S2 in the supplemental material). Cldn1 protein levels were slightly reduced in *ZO-2*$^{-/-}$ EBs (see Fig. S2 in the supplemental material), but the protein was still readily detected at TJs by immunofluorescence microscopy. The localization of other TJ proteins (i.e., Cldn3, occludin, and cingulin) and the distribution of an apical (moesin) and a lateral (E-cadherin) marker were not apparently altered, indicating that cell polarity was unaffected in *ZO-2*$^{-/-}$ EBs (see Fig. S3 in the supplemental material). In contrast to *ZO-2*$^{-/-}$ embryos, the structural appearance of TJs in EBs lacking ZO-2 was normal as assessed by electron microscopy, and no increase in the permeability to lanthanum was detected (see Fig. S4 in the supplemental material).

The analysis of ZO-2$^{-/-}$ EBs thus revealed significant differences with respect to TJ structure and permeability compared to *ZO-2*$^{-/-}$ embryos, suggesting that in *ZO-2*$^{-/-}$ embryos, physiological stress or the maternal uterine environment may affect the structural and/or functional integrity of TJs.

TABLE 2. Apical junctional complex morphology in embryos from *ZO-2*$^{+/-}$ × *ZO-2*$^{+/-}$ matings[a]

Stage	Embryo morphology (no. of embryos)	Characterization of electron-dense plaques at apical junctional complex (no. of sites)			Total no. of sites
		Normal	Rudimentary	Absent	
E6.5	Small (2)	0	4	19	23
E6.5	Normal (5)	48	8	0	56
E7.5	Small (2)	0	7	37	44
E7.5	Normal (3)	25	6	0	31

[a] E6.5 and E7.5 embryo sections were analyzed by transmission electron microscopy to visualize the apical junctional complex. The presence or absence of typical electron-dense plaques (Fig. 10) was quantitated from 23 to 53 sites of cell-cell contact. While electron-dense plaques were always present in embryos of normal size (WT and heterozygous), they were absent in small (*ZO-2*$^{-/-}$) embryos.

DISCUSSION

Members of the ZO protein family were among the first TJ proteins to be identified and have been extensively characterized. In addition to homodimerization (ZO-1) (50) and heterodimerization (ZO-1 with ZO-2 or ZO-3) (55), ZO proteins associate with a multitude of scaffolding proteins found at TJs (reviewed in reference 11), indicating that they form part of an intricate submembranous network. An important role of this scaffold may be to tether ZO TJ transmembrane proteins (i.e., claudins, occludin, and junctional adhesion molecules) to filamentous actin (12, 27), which likely is critical for TJ function. For example, monolayers of renal epithelial cells that express a Cldn16 mutant defective in ZO-1 binding display altered paracellular Mg^{2+} permeability properties (39). ZO proteins also recruit signaling molecules, proteins regulating vesicular

TABLE 3. Quantification of TJ leakiness[a]

Embryo type	No. of embryos examined	No. of TJs	
		Intact	Leaky
WT	5	75	0
ZO-2$^{-/-}$	2	67	8

[a] Lanthanum permeability. E7.5 embryos were postfixed in lanthanum nitrate and processed for transmission electron microscopy. The absence (TJ intact) or presence (TJ leaky) of lanthanum in intercellular spaces adjacent to 75 individual TJs was quantified from WT and *ZO-2*$^{-/-}$ embryos.

trafficking, and transcription factors or coregulators (20, 21, 31, 35, 36). The association of some of these regulatory proteins may, in response to cell-cell adhesion cues, regulate cellular proliferation and differentiation (reviewed in references 35 and 36). ZO proteins are not restricted to TJs or TJ-like structures, but they are also found in gap junctions (25, 33, 42) and the intercalating disc of cardiomyocytes (8). In gap junctions, ZO proteins interact with connexins and possibly regulate connexin trafficking and/or gap junction function (25, 33, 42).

With the exception of ZO-3, which is absent from endothelial cells, ZO proteins are found in most organs of adult mammals and are often coexpressed in particular tissues (26). The relevance of three closely related ZO genes in mammals is unclear. Ablation of ZO protein expression either in cell lines or in mice, indeed, suggests a high degree of redundancy (1, 23, 37, 38, 48, 49). Although often conflicting, these results suggest that individual ZO proteins may be largely dispensable for TJ structure/function or that perhaps their relevance depends on the cell type, extent of protein depletion, or experimental or physiological conditions.

It can be speculated that minor defects in TJ structure or function, as often observed if ZO protein expression is silenced in cells under controlled tissue culture conditions, may lead to more pronounced phenotypes under physiological stress. In addition, the relevance of individual ZO proteins may depend on a particular tissue and/or developmental stage of the organism. It is therefore important to explore the role of ZO proteins in vivo. A first step in this direction has recently been taken with the generation of *ZO-3* KO mice (1). The mice generated by Adachi et al., as well as the *ZO-3*-deficient mice we present in this study, display no apparent phenotype, showing that ZO-3 is dispensable in vivo. In contrast to the *ZO-3* KO animals, however, we show embryonic lethality for *ZO-2*$^{-/-}$ mice, providing for the first time evidence for a critical and nonredundant role for a single ZO protein in mammalian development.

During mouse development, the ZO-1α^- splice variant is incorporated into sites of cell-cell adhesion mediated by E-cadherin at the compacted eight-cell embryonic stage (17). ZO-2 is recruited at the 16-cell stage, and the ZO-1α^+ isoform, cingulin, and Rab13 are incorporated around the 32-cell stage (15). This expression pattern is broadly similar to that of human cleavage stages (18). During these later stages, TJs mature by the segregation of the TJ components from the lateral adherens junctions to establish a permeability barrier associated with blastocoel formation (14, 16, 17). Fluid pumped across the trophectoderm accumulates in the blastocyst to form the blastocoel cavity, a process that likely requires the permeability barrier function of TJs (43). Since *ZO-2*$^{-/-}$ blastocysts can implant into the uterine wall (this study), either fluid accumulation is not required for implantation or ZO-2 is not critical for barrier integrity of the trophectoderm at this stage.

Following implantation, *ZO-2*-deficient embryos fail to complete gastrulation. Embryonic lethality correlates with reduced cell proliferation at E6.5 and increased apoptosis at E7.5, eventually resulting in resorption of the homozygous embryos. The causes for the reduced cellular proliferation and the subsequent cell death are currently unclear, but they are a likely cause for the defect in gastrulation. The finding that expression of the mesoderm marker T is induced in EBs cultured in vitro indicates that mesoderm induction per se may not require ZO-2. Rather, due to the compromised proliferation and the induction of apoptosis, ectoderm cells may never delaminate to form the mesoderm (45).

Neither the localization nor the distribution of other TJ markers (e.g., ZO-1 and ZO-3) is affected in *ZO-2*$^{-/-}$ embryos. Also the distribution of E-cadherin and prominin to the lateral or apical plasma membrane, respectively, is not visibly altered, suggesting that in agreement with earlier studies in MDCK and Eph4 cells (37, 48), apical-basal cell polarity is maintained in the absence of ZO-2. However, given the altered morphology of *ZO-2*$^{-/-}$ embryos and the high background staining compared to tissue culture systems, it would be more difficult to establish minor changes in distribution, as recently reported for MDCK cell monolayers treated with ZO-2 siRNA (23). As observed for *ZO-2*$^{-/-}$ embryos, membrane polarity and the localization of TJ markers are normal in ZO-2-deficient EBs.

Based on the absence of pronounced electron-dense apical junctional plaques, the structural integrity of TJs in *ZO-2*$^{-/-}$ embryos may be compromised. Although at present we do not know if the lack of electron-dense plaques correlates with an absence of TJ strands, as observed in freeze fractures, strands were still found in Eph4 cells where ZO-2 expression was ablated and were lost only in the absence of both ZO-2 and ZO-1 (48). Epithelial-like visceral endoderm *ZO-3*$^{-/-}$ cells retained a normal molecular TJ architecture even when ZO-2 expression was suppressed (1). On the other hand, silencing of ZO-2 in MDCK cells has been reported to result in widened intercellular spaces and increased paracellular permeability (23). Furthermore, nuclear sequestration of ZO-2 has been linked to a reduced junctional stability in MDCK cells (46). Recent evidence also indicates that permeability to ions and larger tracers may not be coupled but may depend on different pathways (22). Considering the large variability of effects on TJ function following depletion of ZO-2 in cultured cells, it is perhaps not surprising that *ZO-2*$^{-/-}$ embryos but not EBs showed apparent structural alterations in TJ morphology and an increased permeability to lanthanum. Given the role of TJs in maintaining unique tissue compartments, developmental arrest may be linked to a defective permeability barrier between the endoderm and the uterine tissue and/or the ectoderm and the proamniotic cavity. Selective alterations in the permeability to specific ions could profoundly affect embryo viability in utero, without being of apparent consequence for cultured EBs. Alternatively, the diffusion of secreted morphogens such as members of the Wnt or transforming growth factor β superfamily may be affected due to changes in tissue permeability, preventing the establishment of gradients required for continued embryonic development. However, while the absence of ZO-2 may affect TJ barriers in the embryo but not in cultured EBs, we cannot rule out that the observed leakiness in *ZO-2*$^{-/-}$ embryos is due to a general cellular deterioration as a result of the decreased proliferation and enhanced apoptosis observed between E6.5 and E7.5.

In addition to a role in TJs, ZO-2 may also regulate gap junctions. ZO proteins are known to bind connexins (19, 30) and have been implicated in the regulation of connexin localization and gap junction formation, localization, and size (25,

33, 42). ZO-2 associates with connexin 43 (Cx43) (44) and, based on colocalization, possibly with other connexins (32). Although gap junctional coupling is critical for blastocyst development (5, 7, 34) and Cx43 contributes to gap junctions during the compaction stage (4, 51), mice with a targeted inactivation of Cx43 develop to full term (41). Several other connexins (i.e., Cx30.3, Cx31, Cx31.1, Cx40, and Cx45) are also expressed in the pre- and postimplantation embryo (10) and may compensate for the loss of Cx43. Given the possible interaction of ZO-2 with several different connexins, gap junction coupling may be more severely affected in *ZO-2*$^{-/-}$ embryos than in embryos that lack a single connexin.

Finally, defects in the regulation of gene expression could contribute to embryonic lethality of *ZO-2*$^{-/-}$ embryos. ZO proteins associate with different transcription factors and regulate gene expression (28, 35). ZO-2, in particular, shuttles between the nucleus and cytoplasm (28, 29) and interacts with several transcription factors, including c-*myc* (24), Jun, Fos, and CCAAT/enhancer-binding protein (6). In the case of c-*myc*, ZO-2 controls the expression of cyclin D1, an important regulator of cell proliferation (24). Alterations in the coordinated expression of genes during development may lead to patterning defects, which often result in embryonic lethality.

Whether the absence of ZO-2 affects paracellular TJ permeability, gap junction connectivity, and/or gene expression, the observation that *ZO-2*$^{-/-}$ ESCs can contribute to the generation of viable chimeric mice (data not shown) implies that ZO-2 may be more critical for extraembryonic functions during early embryonic development than for development of the embryo proper. Indeed, *ZO-2*$^{-/-}$ ESCs can contribute highly to viable adult chimeras, as evidenced by up to 100% agouti coat color. In these chimeric mice, up to 95% of the cells in a specific tissue may lack ZO-2 expression compared to control tissues. Given the epithelial nature of the trophectoderm (54), a requirement for ZO-2 in extraembryonic development is not unexpected.

In summary, while the absence of ZO-3 does not affect embryonic development, embryos lacking ZO-2 fail to complete gastrulation due to loss of cell proliferation and increased cell death. Embryonic lethality of *ZO-2*$^{-/-}$ mice likely results from an extraembryonic requirement for ZO-2 rather than a requisite for development of the embryo proper. ZO-2 therefore exerts a critical function at this developmental stage that cannot be compensated by endogenous ZO-1 or ZO-3, which are also expressed at the egg cylinder stage.

ACKNOWLEDGMENTS

We thank Ray Dunn for helpful discussions, Sathivel Ponniah for expert help with blastocyst injections, and Guo Ke and Zheng Qi for expert assistance with histology and electron microscopy.

This work was supported by the Agency for Science, Technology and Research (A*STAR), Singapore.

REFERENCES

1. **Adachi, M., A. Inoko, M. Hata, K. Furuse, K. Umeda, M. Itoh, and S. Tsukita.** 2006. Normal establishment of epithelial tight junctions in mice and cultured cells lacking expression of ZO-3, a tight-junction MAGUK protein. Mol. Cell. Biol. **26:**9003–9015.
2. **Anderson, J. M., C. M. Van Itallie, and A. S. Fanning.** 2004. Setting up a selective barrier at the apical junction complex. Curr. Opin. Cell Biol. **16:** 140–145.
3. **Balda, M. S., and K. Matter.** 2000. Transmembrane proteins of tight junctions. Semin. Cell Dev. Biol. **11:**281–289.
4. **Barron, D. J., G. Valdimarsson, D. L. Paul, and G. M. Kidder.** 1989. Connexin32, a gap junction protein, is a persistent oogenetic product through preimplantation development of the mouse. Dev. Genet. **10:**318–323.
5. **Becker, D. L., W. H. Evans, C. R. Green, and A. Warner.** 1995. Functional analysis of amino acid sequences in connexin43 involved in intercellular communication through gap junctions. J. Cell Sci. **108:**1455–1467.
6. **Betanzos, A., M. Huerta, E. Lopez-Bayghen, E. Azuara, J. Amerena, and L. Gonzalez-Mariscal.** 2004. The tight junction protein ZO-2 associates with Jun, Fos and C/EBP transcription factors in epithelial cells. Exp. Cell Res. **292:**51–66.
7. **Bevilacqua, A., R. Loch-Caruso, and R. P. Erickson.** 1989. Abnormal development and dye coupling produced by antisense RNA to gap junction protein in mouse preimplantation embryos. Proc. Natl. Acad. Sci. USA **86:**5444–5448.
8. **Borrmann, C. M., C. Grund, C. Kuhn, I. Hofmann, S. Pieperhoff, and W. W. Franke.** 2006. The area composita of adhering junctions connecting heart muscle cells of vertebrates. II. Colocalizations of desmosomal and fascia adhaerens molecules in the intercalated disk. Eur. J. Cell Biol. **85:**469–485.
9. **Borrmann, C. M., C. Mertens, A. Schmidt, L. Langbein, C. Kuhn, and W. W. Franke.** 2000. Molecular diversity of plaques of epithelial-adhering junctions. Ann. N Y. Acad. Sci. **915:**144–150.
10. **Davies, T. C., K. J. Barr, D. H. Jones, D. Zhu, and G. M. Kidder.** 1996. Multiple members of the connexin gene family participate in preimplantation development of the mouse. Dev. Genet. **18:**234–243.
11. **Fanning, A. S., and J. M. Anderson.** 1999. PDZ domains: fundamental building blocks in the organization of protein complexes at the plasma membrane. J. Clin. Investig. **103:**767–772.
12. **Fanning, A. S., B. J. Jameson, L. A. Jesaitis, and J. M. Anderson.** 1998. The tight junction protein ZO-1 establishes a link between the transmembrane protein occludin and the actin cytoskeleton. J. Biol. Chem. **273:**29745–29753.
13. **Farquhar, M. G., and G. E. Palade.** 1963. Junctional complexes in various epithelia. J. Cell Biol. **17:**375.
14. **Fleming, T. P., M. R. Ghassemifar, and B. Sheth.** 2000. Junctional complexes in the early mammalian embryo. Semin. Reprod. Med. **18:**185–193.
15. **Fleming, T. P., M. Hay, Q. Javed, and S. Citi.** 1993. Localisation of tight junction protein cingulin is temporally and spatially regulated during early mouse development. Development **117:**1135–1144.
16. **Fleming, T. P., J. McConnell, M. H. Johnson, and B. R. Stevenson.** 1989. Development of tight junctions de novo in the mouse early embryo: control of assembly of the tight junction-specific protein, ZO-1. J. Cell Biol. **108:** 1407–1418.
17. **Fleming, T. P., T. Papenbrock, I. Fesenko, P. Hausen, and B. Sheth.** 2000. Assembly of tight junctions during early vertebrate development. Semin. Cell Dev. Biol. **11:**291–299.
18. **Ghassemifar, M. R., J. J. Eckert, F. D. Houghton, H. M. Picton, H. J. Leese, and T. P. Fleming.** 2003. Gene expression regulating epithelial intercellular junction biogenesis during human blastocyst development in vitro. Mol. Hum. Reprod. **9:**245–252.
19. **Giepmans, B. N.** 2004. Gap junctions and connexin-interacting proteins. Cardiovasc. Res. **62:**233–245.
20. **Gonzalez-Mariscal, L., A. Betanzos, and A. Avila-Flores.** 2000. MAGUK proteins: structure and role in the tight junction. Semin. Cell Dev. Biol. **11:**315–324.
21. **Gonzalez-Mariscal, L., A. Betanzos, P. Nava, and B. E. Jaramillo.** 2003. Tight junction proteins. Prog. Biophys. Mol. Biol. **81:**1–44.
22. **Herman, R. E., E. G. Makienko, M. G. Prieve, M. Fuller, M. E. Houston, Jr., and P. H. Johnson.** 2007. Phage display screening of epithelial cell monolayers treated with EGTA: identification of peptide FDFWITP that modulates tight junction activity. J. Biomol. Screen. **12:**1091–1101
23. **Hernandez, S., B. Chavez Munguia, and L. Gonzalez-Mariscal.** 2007. ZO-2 silencing in epithelial cells perturbs the gate and fence function of tight junctions and leads to an atypical monolayer architecture. Exp. Cell Res. **313:**1533–1547.
24. **Huerta, M., R. Munoz, R. Tapia, E. Soto-Reyes, L. Ramirez, F. Recillas-Targa, L. Gonzalez-Mariscal, and E. Lopez-Bayghen.** 2007. Cyclin D1 is transcriptionally down-regulated by ZO-2 via an E box and the transcription factor c-Myc. Mol. Biol. Cell **18:**4826–4836.
25. **Hunter, A. W., R. J. Barker, C. Zhu, and R. G. Gourdie.** 2005. ZO-1 alters connexin43 gap junction size and organization by influencing channel accretion. Mol. Biol. Cell **16:**5686–5698.
26. **Inoko, A., M. Itoh, A. Tamura, M. Matsuda, M. Furuse, and S. Tsukita.** 2003. Expression and distribution of ZO-3, a tight junction MAGUK protein, in mouse tissues. Genes Cells **8:**837–845.
27. **Itoh, M., M. Furuse, K. Morita, K. Kubota, M. Saitou, and S. Tsukita.** 1999. Direct binding of three tight junction-associated MAGUKs, ZO-1, ZO-2, and ZO-3, with the COOH termini of claudins. J. Cell Biol. **147:**1351–1363.
28. **Jaramillo, B. E., A. Ponce, J. Moreno, A. Betanzos, M. Huerta, E. Lopez-Bayghen, and L. Gonzalez-Mariscal.** 2004. Characterization of the tight junction protein ZO-2 localized at the nucleus of epithelial cells. Exp. Cell Res. **297:**247–258.
29. **Kausalya, P. J., D. C. Phua, and W. Hunziker.** 2004. Association of ARVCF with zonula occludens (ZO)-1 and ZO-2: binding to PDZ-domain proteins

and cell-cell adhesion regulate plasma membrane and nuclear localization of ARVCF. Mol. Biol. Cell **15:**5503–5515.
30. **Kausalya, P. J., M. Reichert, and W. Hunziker.** 2001. Connexin45 directly binds to ZO-1 and localizes to the tight junction region in epithelial MDCK cells. FEBS Lett. **505:**92–96.
31. **Kohler, K., and A. Zahraoui.** 2005. Tight junction: a co-ordinator of cell signalling and membrane trafficking. Biol. Cell **97:**659–665.
32. **Kojima, T., Y. Kokai, H. Chiba, M. Yamamoto, Y. Mochizuki, and N. Sawada.** 2001. Cx32 but not Cx26 is associated with tight junctions in primary cultures of rat hepatocytes. Exp. Cell Res. **263:**193–201.
33. **Laing, J. G., B. C. Chou, and T. H. Steinberg.** 2005. ZO-1 alters the plasma membrane localization and function of Cx43 in osteoblastic cells. J. Cell Sci. **118:**2167–2176.
34. **Lee, S., N. B. Gilula, and A. E. Warner.** 1987. Gap junctional communication and compaction during preimplantation stages of mouse development. Cell **51:**851–860.
35. **Matter, K., and M. S. Balda.** 2007. Epithelial tight junctions, gene expression and nucleo-junctional interplay. J. Cell Sci. **120:**1505–1511.
36. **Matter, K., and M. S. Balda.** 2003. Signalling to and from tight junctions. Nat. Rev. Mol. Cell Biol. **4:**225–236.
37. **McNeil, E., C. T. Capaldo, and I. G. Macara.** 2006. Zonula occludens-1 function in the assembly of tight junctions in Madin-Darby canine kidney epithelial cells. Mol. Biol. Cell **17:**1922–1932.
38. **Medina, R., C. Rahner, L. L. Mitic, J. M. Anderson, and C. M. Van Itallie.** 2000. Occludin localization at the tight junction requires the second extracellular loop. J. Membr. Biol. **178:**235–247.
39. **Müller, D., P. J. Kausalya, F. Claverie-Martin, I. C. Meij, P. Eggert, V. Garcia-Nieto, and W. Hunziker.** 2003. A novel claudin 16 mutation associated with childhood hypercalciuria abolishes binding to ZO-1 and results in lysosomal mistargeting. Am. J. Hum. Genet. **73:**1293–1301.
40. **Poliak, S., S. Matlis, C. Ullmer, S. S. Scherer, and E. Peles.** 2002. Distinct claudins and associated PDZ proteins form different autotypic tight junctions in myelinating Schwann cells. J. Cell Biol. **159:**361–372.
41. **Reaume, A. G., P. A. de Sousa, S. Kulkarni, B. L. Langille, D. Zhu, T. C. Davies, S. C. Juneja, G. M. Kidder, and J. Rossant.** 1995. Cardiac malformation in neonatal mice lacking connexin43. Science **267:**1831–1834.
42. **Segretain, D., C. Fiorini, X. Decrouy, N. Defamie, J. R. Prat, and G. Pointis.** 2004. A proposed role for ZO-1 in targeting connexin 43 gap junctions to the endocytic pathway. Biochimie **86:**241–244.
43. **Sheth, B., J. J. Fontaine, E. Ponza, A. McCallum, A. Page, S. Citi, D. Louvard, A. Zahraoui, and T. P. Fleming.** 2000. Differentiation of the epithelial apical junctional complex during mouse preimplantation development: a role for rab13 in the early maturation of the tight junction. Mech. Dev. **97:**93–104.
44. **Singh, D., J. L. Solan, S. M. Taffet, R. Javier, and P. D. Lampe.** 2005. Connexin 43 interacts with zona occludens-1 and -2 proteins in a cell cycle stage-specific manner. J. Biol. Chem. **280:**30416–30421.
45. **Tam, P. P., and D. A. Loebel.** 2007. Gene function in mouse embryogenesis: get set for gastrulation. Nat. Rev. Genet. **8:**368–381.
46. **Traweger, A., C. Lehner, A. Farkas, I. A. Krizbai, H. Tempfer, E. Klement, B. Guenther, H. C. Bauer, and H. Bauer.** 31 October 2007. Nuclear zonula occludens-2 alters gene expression and junctional stability in epithelial and endothelial cells. Differentiation. [Epub ahead of print.] doi: 10.1111/j.1432-0436.2007.00227.x.
47. **Tsukita, S., M. Furuse, and M. Itoh.** 2001. Multifunctional strands in tight junctions. Nat. Rev. Mol. Cell Biol. **2:**285–293.
48. **Umeda, K., J. Ikenouchi, S. Katahira-Tayama, K. Furuse, H. Sasaki, M. Nakayama, T. Matsui, S. Tsukita, M. Furuse, and S. Tsukita.** 2006. ZO-1 and ZO-2 independently determine where claudins are polymerized in tight-junction strand formation. Cell **126:**741–754.
49. **Umeda, K., T. Matsui, M. Nakayama, K. Furuse, H. Sasaki, M. Furuse, and S. Tsukita.** 2004. Establishment and characterization of cultured epithelial cells lacking expression of ZO-1. J. Biol. Chem. **279:**44785–44794.
50. **Utepbergenov, D. I., A. S. Fanning, and J. M. Anderson.** 2006. Dimerization of the scaffolding protein ZO-1 through the second PDZ domain. J. Biol. Chem. **281:**24671–24677.
51. **Valdimarsson, G., and G. M. Kidder.** 1995. Temporal control of gap junction assembly in preimplantation mouse embryos. J. Cell Sci. **108:**1715–1722.
52. **Van Itallie, C. M., and J. M. Anderson.** 2006. Claudins and epithelial paracellular transport. Annu. Rev. Physiol. **68:**403–429.
53. **Van Itallie, C. M., and J. M. Anderson.** 2004. The molecular physiology of tight junction pores. Physiology **19:**331–338.
54. **Wiley, L. M., G. M. Kidder, and A. J. Watson.** 1990. Cell polarity and development of the first epithelium. Bioessays **12:**67–73.
55. **Wittchen, E. S., J. Haskins, and B. R. Stevenson.** 1999. Protein interactions at the tight junction. Actin has multiple binding partners, and ZO-1 forms independent complexes with ZO-2 and ZO-3. J. Biol. Chem. **274:**35179–35185.